Journal of Solid State Chemistry 184 (2011) 1956–1962

Contents lists available at ScienceDirect

Journal of Solid State Chemistry

journal homepage: www.elsevier.com/locate/jssc

One-pot synthesis, optical property and self-assembly of monodisperse silver nanospheres

Aiwei Tang [a,b,*], Shengchun Qu [b], Yanbing Hou [c], Feng Teng [c,**], Yongsheng Wang [c], Zhanguo Wang [b]

[a] Department of Chemistry, School of Science, Beijing JiaoTong University, Beijing 100044, China
[b] Key Laboratory of Semiconductor Materials Science, Institute of Semiconductors, Chinese Academy of Sciences, Beijing 100083, China
[c] Key Laboratory of Luminescence and Optical Information, Ministry of Education, Institute of Optoelectronic Technology, Beijing JiaoTong University, Beijing 100044, China

ARTICLE INFO

Article history:
Received 15 February 2011
Received in revised form
28 April 2011
Accepted 29 May 2011
Available online 7 June 2011

Keywords:
Ag nanospheres
Self-assembly
Optical property
Superlattice structures

ABSTRACT

High-quality spherical silver (Ag) nanocrystals have been synthesized by using a one-pot approach, in which pre-synthesis of organometallic precursors is not required. This reaction involves the thermolysis of a mixed solution of silver acetate and *n*-dodecanethiol in a non-coordinating organic solvent. The size of the as-obtained Ag nanospheres can be controlled by adjusting the reaction time, reaction temperature and the amount of silver acetate added. The growth and nucleation process of the resultant Ag nanospheres have been studied by employing UV–vis absorption spectra and transmission electron microscopy (TEM) images. Furthermore, these Ag nanospheres have good self-assembly behaviors, and they are easily self-assembled into two- or three-dimensional superlattice structures due to the bundling and interdigitation of thiolate molecules adsorbed on Ag nanospheres. This one-pot synthetic procedure is simple and highly reproducible, which may be extended to prepare other noble-metal nanocrystals.

1. Introduction

In the past few decades, colloidal nanocrystals have attracted much attention due to their potential applications in optoelectronic and biological fields [1–4]. Among these well-known colloidal nanocrystals, noble-metal nanocrystals may be one of the most important category. To date, these noble-metal nanocrystals have been widely used in the fields of catalysis [5], memory devices [6,7], and surface-enhanced Raman scattering (SERS) [8,9], and also used as building blocks for nanocrystal assemblies [10]. Up to now, a large number of physical and chemical synthetic methods have been explored to effectively control the size and morphology of noble-metal nanocrystals, such as polyol process [11,12], aerosol technique [13], thermolysis of a single-source organometallic precursor [14,15], surfactant-promoted reductive route [16,17], seed-growth method [18] and so on. These strategies make it possible to produce high-quality metal nanocrystals with uniform size and different shapes ranging spheres to wires, rods, disks, cubes and prisms [11–18]. As an important member of metal nanocrystals, silver (Ag) nanocrystals have been extensively studied and are of particular interest because of their unusual properties and applications presumably associated with their morphologies and size [19,20]. In those aforementioned non-aqueous notable approaches, alkanethiol often played an important role in producing monodisperse Ag nanocrystals. Interestingly, the thiolate molecules adsorbed on the nanocrystals' surface not only acted as the protective layer of the nanocrystals from aggregation but also directed the Ag nanocrystals to assemble into two- or three-dimensional (2D or 3D) superlattice structures [17,21].

Although so much success has been made in the synthesis of Ag nanocrystals, yet it is still challenging to develop a simple but low-cost technique for preparing uniform and large-scale Ag nanocrystals with tunable size less than 10 nm. The size of the metal nanocrystals that can be self-assembled into superlattice structures is usually smaller than 10 nm, and it is in this size range that some exciting and unusual physical properties are enhanced [22]. In this paper, we reported a facile one-pot reaction for synthesis of Ag nanospheres with excellent control of their size at high temperature ($>200\ ^{\circ}C$). This process was designed by thermolysis of a mixture of silver acetate and *n*-dodecanethiol in a high boiling-point solvent [23,24]. This synthetic process does not need any extra steps for preparing metal precursors. Importantly, this method represents a highly reproducible approach for producing large-scale and high-quality Ag nanocrystals. The size of the as-obtained Ag nanospheres could be conveniently tailored via adjusting the reaction time, temperature and the precursor ratios. Due to the interaction between the neighboring nanospheres, the Ag nanospheres have a high tendency to be self-assembled into highly ordered superlattice structures.

* Corresponding author at: Department of Chemistry, School of Science, Beijing JiaoTong University, Beijing 100044, China.
** Corresponding author.
E-mail addresses: awtang@bjtu.edu.cn (A. Tang), fteng@bjtu.edu.cn (F. Teng).

0022-4596/$ - see front matter © 2011 Elsevier Inc. All rights reserved.
doi:10.1016/j.jssc.2011.05.041

2. Materials and methods

2.1. Materials

Silver acetate (Ag(Ac), Sinopharm Chemical Reagent Co., Ltd., China, ≥99%), 1-Octadecene (ODE, J&K Chemical Ltd., 90%), *n*-dodecanethiol (DDT, Sinopharm Chemical Reagent Co., Ltd., China, 98%) were used as purchased without further purification. Other solvents such as ethanol and chloroform were commercially available products in analytical grade, which were purchased from Beijing Chemical Reagent, China.

2.2. Synthesis of Ag nanospheres

In a typical synthesis of sample A, 15 mmol of Ag(Ac) was dissolved in 10 ml of DDT and 20 ml of ODE. The mixture was degassed by nitrogen gas for about 20 min. Then the mixture was heated up to 200 °C and kept at the temperature for several hours. Aliquots were extracted from the mixture at different reaction intervals for monitoring the shape and size evolutions of the resultant samples. Right after the reaction, the aliquots solution was collected and then centrifuged at 6000 rpm for 10 min. The supernatant was discarded and the precipitation was fully dispersed in chloroform, and then precipitated by adding some ethanol, following by centrifugation at 6000 rpm for 10 min. The precipitation and washing procedures were repeated three times to remove surfactant residuals, un-reacted reactants and the by-products. Finally, the resultant Ag nanospheres obtained at different reaction time were re-dispersed into chloroform or dried in vacuum for next characterization. Different-sized Ag nanospheres (samples B and C) were also synthesized using the same conditions as the process for sample A. For the sake of convenience, the detailed experimental conditions are summarized in Table 1.

2.3. Sample characterization

The morphology of the samples was studied using a Hitachi-7650 transmission electron microscope operating at an accelerating voltage of 100 kV. High-resolution transmission electron microscopy (HRTEM) images and selected-area electron diffraction (SAED) patterns were recorded using a JEM-2010 transmission electron microscope working at an accelerating voltage of 200 kV. The X-ray photoelectron spectroscopic (XPS) measurements were performed on a VG ESCALAB 220i-XL spectrometer with a 300 W Al$K\alpha$ radiation source. All binding energies for different elements were calibrated with respect to C 1*s* line at 284.8 eV from the contaminant carbon. The thermogravimetric analysis (TGA) and differential thermal analysis (DTA) were measured using a NETZSCH TG209 F3 instrument. Crystal structure of the samples was measured using Bruker D8 Discover X-ray Diffractometer with a Cu$K\alpha$ radiation source ($\lambda = 1.54056$ Å). Fourier transform infrared spectra (FTIR) were collected using a Varian Excalibur 3100 spectrometer. The UV–vis absorption spectra of the Ag nanospheres in chloroform were obtained on a Shimadzu-UV 3101 spectrophotometer. All the measurements were carried out under ambient conditions at room temperature.

Table 1
Experimental conditions for preparing different-sized Ag nanospheres at different reaction temperatures and amounts of Ag(Ac).

Samples	Amount of Ag(Ac) (mmol)	Reaction temperature (°C)
Sample A	15	200
Sample B	15	240
Sample C	3	240

3. Results and discussion

In this work, Ag nanospheres were obtained by heating silver acetate and *n*-dodecanethiol in a non-coordinating solvent (ODE) at high temperature, in which DDT was used as a surface-capping ligand, and ODE acted as a solvent to allow the reaction to be performed. In order to study the effects of reaction conditions on the size of Ag nanospheres, different Ag nanospheres were prepared at different reaction temperatures and different precursor ratios. Generally speaking, metal precursors can react with DDT initially to form an intermediate complex [25]. Herein, the reaction of Ag(Ac) and DDT leads to the formation of intermediate complex, as demonstrated by the color change from turbid suspension to a yellow and transparent mixture at early stage. Afterwards, the color of the system changed from yellow to dark-brown while the reaction was going on, and finally black nanocrystal ink was obtained. The schematic illustration of the synthetic procedure for Ag nanospheres is shown in Fig. 1. The intermediate products obtained at the initial stage can be identified as the formation of Ag-thiolate $[Ag_m(SC_{12}H_{25})_n]$ precursor with a layered structure, which is confirmed by the sharp diffraction peaks of small-angle XRD patterns of the sample taken from at the beginning of the reaction (see Figure. S1 in Supporting information). The sharp diffraction peaks at lower angles correspond to successive orders of diffractions from layered structure of Ag-thiolate observed previously by Wu and co-workers [14]. During the next refluxing process, the thermal decomposition of the resultant Ag-thiolate precursor took place, in which the Ag ions could be reduced by the thiolate group with the formation of disulfide [14]. The following reaction seems to be responsible for the synthesis of Ag nanocrystals:

$$Ag(CH_3COO) + 2C_{12}H_{25}SH \rightarrow Ag + C_{12}H_{25}SSC_{12}H_{25} + CH_3COOH.$$

As a result, the monodisperse Ag nanospheres were obtained after washing and precipitation process (as shown in Fig. 1).

In order to obtain detailed information of the thermal behavior of Ag-thiolate precursor, the TGA and DTA analyses of the Ag

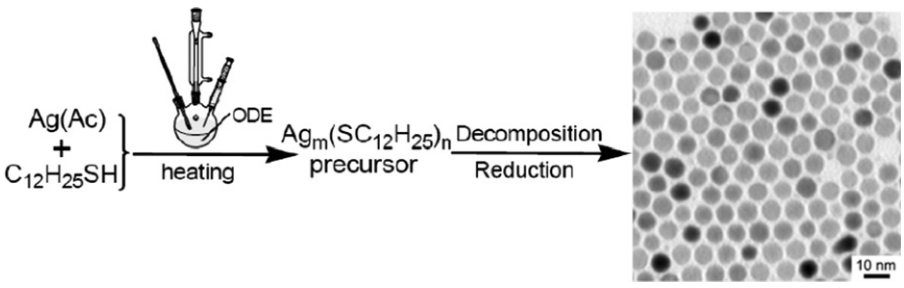

Fig. 1. A schematic illustration of the process for preparing monodisperse Ag nanospheres.

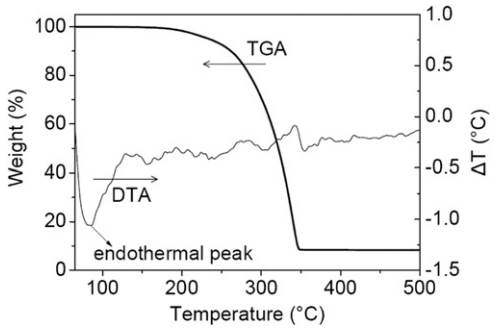

Fig. 2. Typical TGA and DTA curves of sample A.

nanospheres are given in Fig. 2. A rapid weight loss is observed mainly in the temperature range from 250 to 350 °C. Since the boiling point of *n*-dodecanethiol is in the range 266–283 °C, the above weight loss observed in TGA curve may be caused by the evaporation and volatilization of *n*-dodecanethiol or other organic molecules [26]. On the other hand, an endothermal peak is observed at about 90 °C, which may be attributed to the desorption of dodecanethiol molecules from the surface of Ag nanospheres [27], and another endothermal peak at about 150 °C, probably due to the reorganization of the chains of dodecanethiol molecules. The broad exothermal range may result from the dissociation of the ligands from the core of the nanospheres and the evaporation of rudimental ODE.

The nucleation and growth process of the as-obtained Ag nanospheres was characterized by using TEM images. The TEM results of sample A extracted at different reaction time are presented in Fig. 3. The aforementioned results indicate that the intermediate polymeric precursor $[Ag_m(SC_{12}H_{25})_n]$ was formed at early stage through the reaction between Ag(Ac) and DDT. As shown in Fig. 3(a), irregularly shaped crystals appeared in the samples extracted at 20 min. In fact, some very small particles are observed, and they are encapsulated in the organic phase. It is believed that the accumulation of monomer species took place as partially demonstrated by the transition of the mixture color from yellow to dark-brown, which eventually led to nucleation of nanocrystals upon supersaturation. After nucleation, the monomer species were adsorbed onto the surface of Ag nanospheres, promoting the progressive growth of the nanocrystals, which has been studied in the case of Cu_2S nanocrystals [24,28]. Fig. 3(b) shows the TEM images of sample A collected at 60 min, and the Ag nanospheres are connected to a network structure with a larger area due to the cohesive interaction of layered thiolate molecules adsorbed on the surface of Ag nanospheres. As the reaction time was prolonged to 100 min, the $[Ag_m(SC_{12}H_{25})_n]$ complex was partially consumed, uniform Ag nanospheres with a mean diameter of 4.0 ± 0.4 nm are obtained, as shown in Fig. 3(c). Fig. 3(d) gives the HRTEM image of Ag nanospheres obtained at 100 min, careful inspection suggests that the lattice fringes of this sample are clearly resolved, confirming their crystallinity. Interestingly, the Ag nanospheres can be self-assembled into hexagonal close-packed arrays with one particle surrounded symmetrically by the other six particles. Further prolonging the reaction time to 180 min allowed the average diameter of the Ag nanospheres to increase from 4.0 ± 0.4 nm (100 min) to 5.4 ± 0.4 nm (180 min), but the shape of the samples still remained in spherical, as depicted in Fig. 3(e). The corresponding SAED pattern of sample A obtained at 180 min has been performed, which is given in Fig. 3(f). All the diffraction rings can be assigned to (1 1 1), (2 0 0), (2 2 0) and (3 1 1) reflections, confirming the formation of face-centered cubic silver (JCPDS Card no.87-0597) [9]. It is noted that some well-resolved diffraction spots are observed in the SAED pattern, demonstrating the formation of metallic silver.

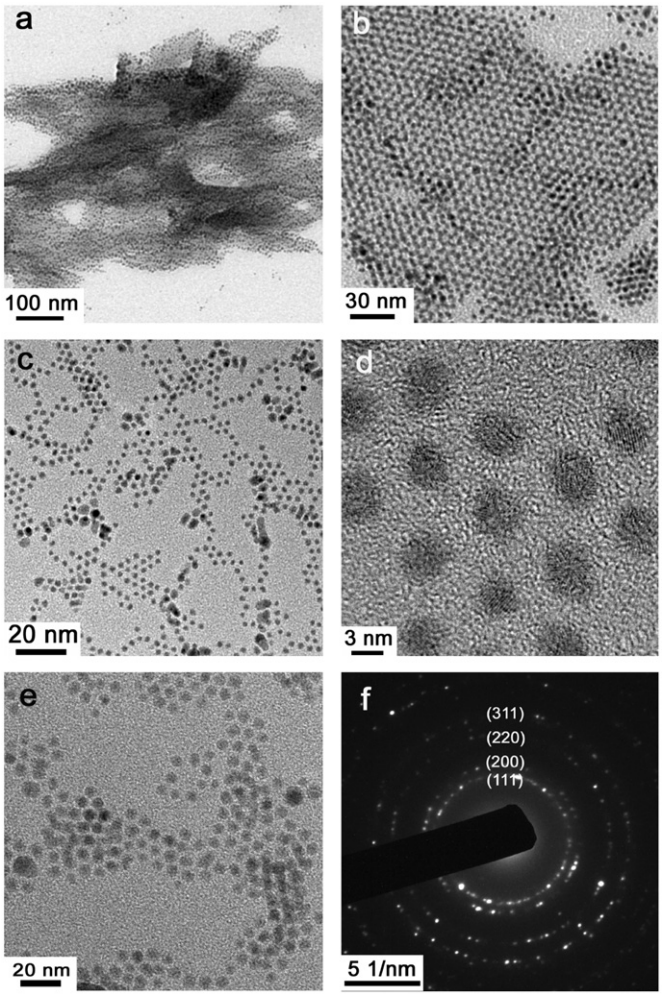

Fig. 3. TEM images of sample A extracted at different reaction time: (a) 20 min; (b) 60 min; (c, d) 100 min; (e)180 min and (f) the corresponding SAED pattern.

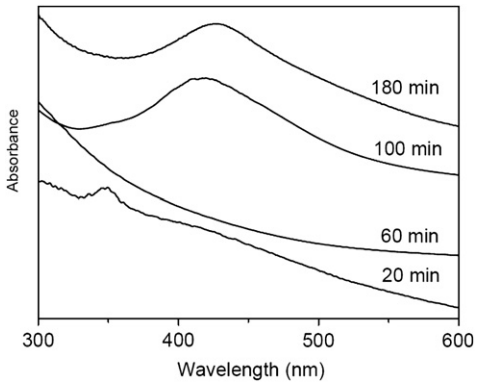

Fig. 4. Temporal evolution of UV–vis absorption spectra of sample A.

UV–vis spectroscopy was employed to monitor the optical property of the Ag nanospheres during their nucleation and growth process. Fig. 4 shows the temporal evolution of the absorption spectra for sample A. For the sample A obtained at 20 min, an absorption band at 348 nm is observed, which may be related with the formation of dominant presence of $[Ag_m(SC_{12}H_{25})_n]$ complex. As the Ag-thiolate precursor is consumed, the absorption band at 348 nm disappears for sample A collected after 60 min, indicating the formation of monomer species. After nucleation, the growth of Ag nanospheres makes the absorption of Ag nanospheres become

apparent. After reaction for 100 min, an obvious absorption band at 427 nm appears, which is typical of the absorption of metallic Ag nanospheres. This absorption band is attributed to the excitation of the surface plasma resonance (SPR) of Ag nanospheres [12]. A narrow and symmetric absorption peak implies that the size of the Ag nanospheres is very uniform [9].

In order to get a molecular level understanding of the capping ligands on the nanocrystal surface, FTIR spectroscopies of samples A and C were measured, which are shown in Fig. 5. It is found that both samples have two sharp bands at 2916 and 2848 cm^{-1} due to asymmetric methyl stretching vibration and the asymmetric and symmetric methylene stretching vibration from the DDT molecule [28]. The band at 1467 cm^{-1} can be assigned to methylene scissoring of DDT [29]. The absence of the band at 2577 cm^{-1} arising from the *S–H* vibrations of DDT suggests the deprotonation of DDT, and this indicates that DDT may serve as the capping ligand for the growth of Ag nanospheres [25,28].

XPS analysis was employed to detect the oxidation state and composition of the as-obtained Ag nanospheres. The XPS survey spectrum, Ag 3*d* signals and S 2*p* signals of sample A are shown in Fig. 6(a)–(c), respectively. The XPS survey spectrum shown in Fig. 6(a) confirms the formation of Ag nanospheres and reveals the presence of thiolate ligands on the surface of the as-obtained Ag nanospheres. The peak position and peak to peak separation (about 6 eV) are the judgement standard for indentifying the oxidation state of Ag [29]. As shown in Fig. 6(b), the core levels of Ag $3d_{5/2}$ and Ag $3d_{3/2}$ located at 373.8 and 367.8 eV correspond to an Ag(0) oxidation state, which is in agreement with those of previous reported values [29,30]. In Fig. 6(c), the S 2*p* core level signal can be resolved into two peaks at 162.6 and 161.3 eV, which are assigned to the binding energy of S $2p_{1/2}$ and S $2p_{3/2}$, respectively. This result matches well with the values for chemically bound thiolate sulfur in previous reports [31,32]. The absence of the peak above 163 eV excludes the possibility of the presence of free alkanethiol, disulfides and oxidized sulfur [29,32].

XRD patterns were used to determine the atomic structure of the final product, which may further confirm the formation of Ag nanospheres. Representative XRD patterns of Ag nanospheres (sample A and sample B) are given in Fig. 7. For both of the samples, the four diffraction peaks correspond to (1 1 1), (2 0 0), (2 2 0) and (3 1 1) reflections, indicating that the formation of Ag particles with face-centered cubic structure (JCPDS Card no.87-0597, lattice parameter $a=4.0862$ Å) [14]. This result matches well with the SAED results. In addition, no other species, such as Ag_2S or Ag_2O, is observed in the as-obtained samples. The above XPS analysis and the XRD results thus clearly prove the formation of Ag nanospheres with the surface passivation of DDT.

According to previous reports, the nanocrystal size and shape can be controlled using the following parameters as the variables: reaction temperature, reaction time and ratio of ligand to metal

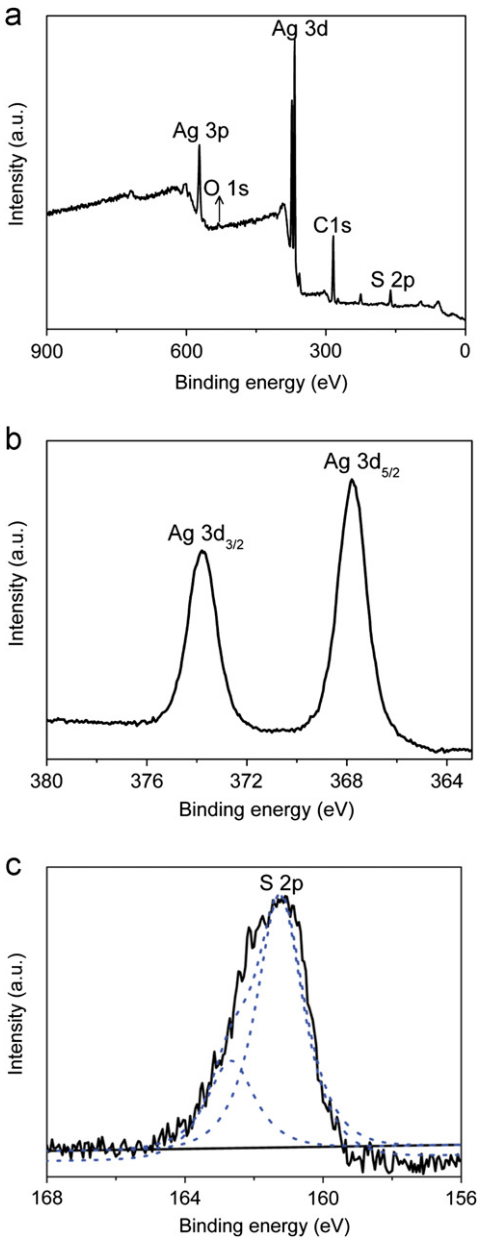

Fig. 6. Representative XPS spectra of Ag nanospheres (sample A): (a) survey spectrum; (b) Ag 3*d* core level and (c) S 2*p* core level with the experimental result (solid line) and the fitting result (dotted line).

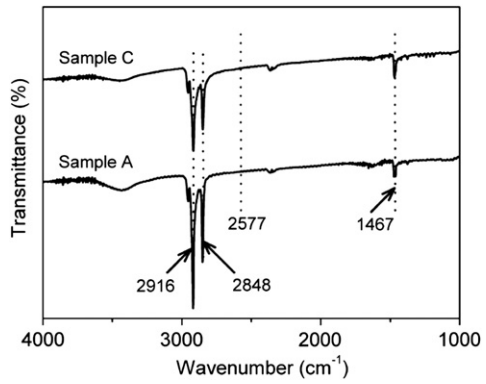

Fig. 5. FTIR spectra of sample A and sample C.

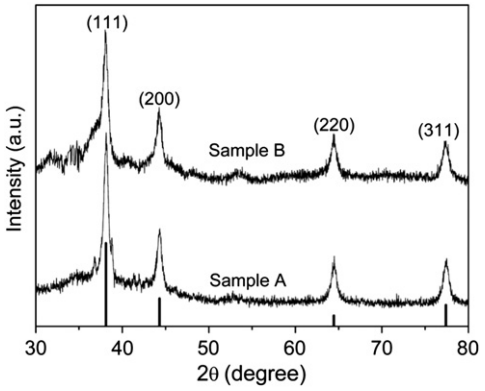

Fig. 7. XRD patterns of sample A and sample B.

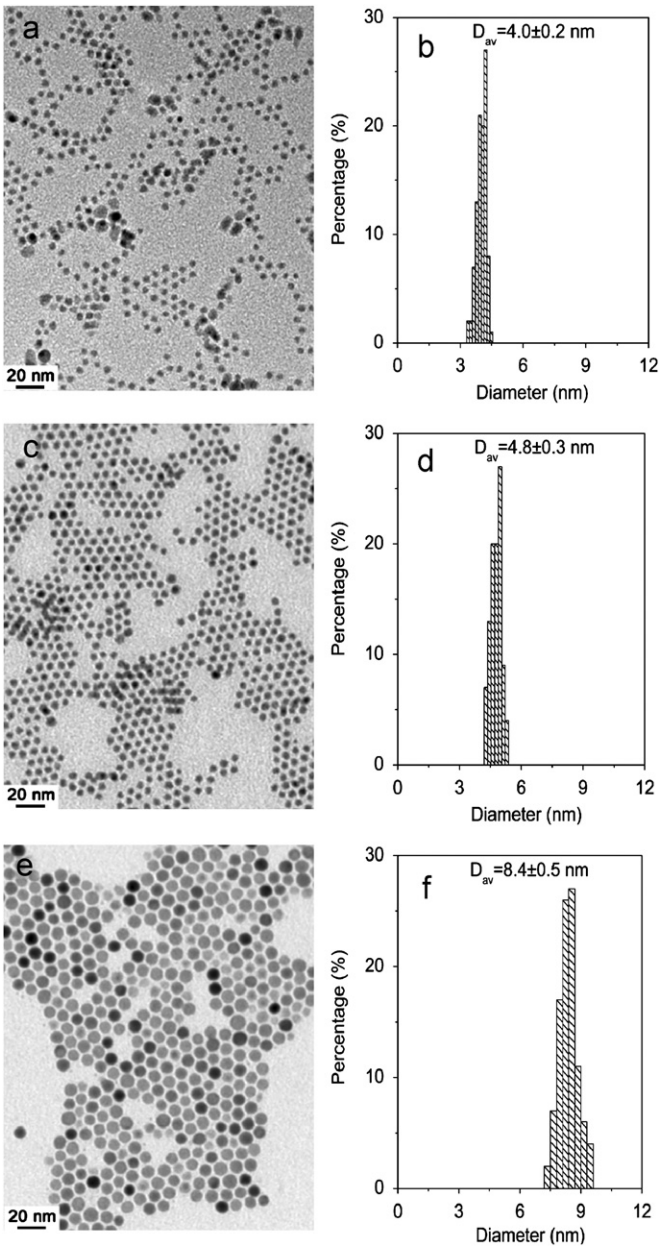

Fig. 8. TEM images and the corresponding size distribution histogram of Ag nanospheres with different reaction conditions at 100 min: (a, b) sample A; (c, d) sample B; and (e, f) sample C.

salt [24,28,31]. Fig. 8 presents the TEM images and the corresponding size distribution histograms of the as-obtained Ag nanospheres by changing the reaction temperature and the ratio of Ag(Ac) to DDT. As the reaction temperature was raised from 200 to 240 °C while all other reaction conditions were kept the same, the mean size of the as-obtained Ag nanospheres was increased from 4.0 ± 0.2 nm (sample A) to 4.8 ± 0.3 nm (sample B). The particles display a narrow size distribution and an overall spherical shape. This indicates that the reduction of the Ag-thiolate precursors and the growth of Ag nanospheres can be accelerated by increasing the reaction temperature, which is characteristic for a decomposition reaction. At a higher temperature, the stability of the intermediate complexes is decreased, which provides more monomer species to enhance the rates of both nanocrystal nucleation and growth [33,34]. On the other hand, increasing the temperature may weaken the binding of the surfactants to the surface of the nanocrystals, which may quicken the growth of the nanocrystals [24]. In addition, when the reaction temperature was kept at 240 °C, the amount of Ag(Ac) was decreased to 20% of that used for sample B, the mean size of sample C was increased to 8.4 ± 0.5 nm with a narrow size distribution ($< 10\%$), but the spherical shape was still unchanged. This suggests that the amount of the Ag(Ac) present in the solution is important for controlling the size of Ag nanospheres. Therefore, the size of the as-obtained Ag nanospheres can be easily controlled by varying the reaction conditions.

The self-assembly behaviors of noble-metal nanocrystals were reported before, in which the noble-metal nanocrystals could be self-assembled into highly ordered superlattice structures due to the narrow size distribution or the cohesive interaction through interdigitation or interpenetration of the capping ligand [35–41]. With respect to the Ag nanospheres in this work, almost perfect 3D superlattices were also observed by slow evaporation of carrier solvent from a dense solution, which was deposited onto carbon-coated Cu grids. Fig. 9 displays the high- and low-resolution TEM images of Ag nanocrystal superlattices (sample B). As shown in Fig. 9(b), irregularly shaped 3D superlattices with clearly defined edges are observed, and the domain size of the superlattice structures can reach up to several micrometers. Fig. 9(a) and (c) represent the magnified images of the superlattice edge in Fig. 9(b). This nanocrystal superlattice is remarkable in the perfect arrangement of monodispersed Ag nanospheres [38]. As stated in previous reports, the presence of excess alkylthiol played an important role in the Ag or Au nanocrystal superlattice formation due to the cohesive interaction through interdigitation or interpenetration of alkyl chains of thiol molecules [21,22]. Herein, the adjacent Ag nanospheres are separated by a distance of less than 3 nm estimated from TEM results in Fig. 9(c). The length of alkanethiol

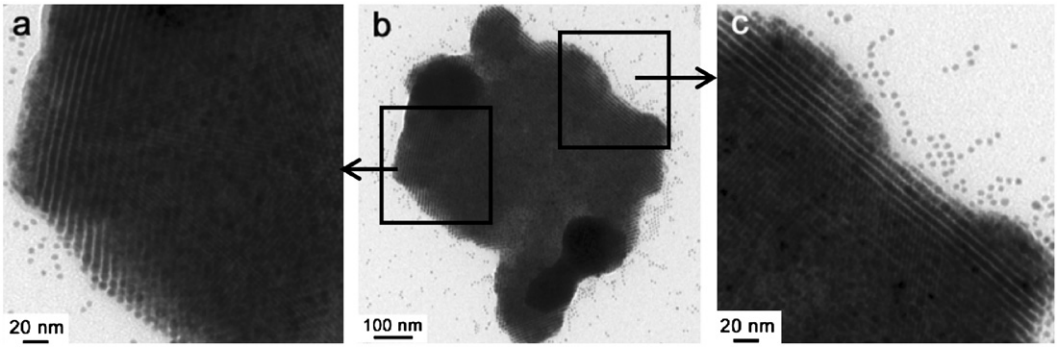

Fig. 9. TEM images of typical superlattice structures of sample B obtained at 100 min: (b) a low-magnification image, and (a, c) magnified images of superlattice edges from (b).

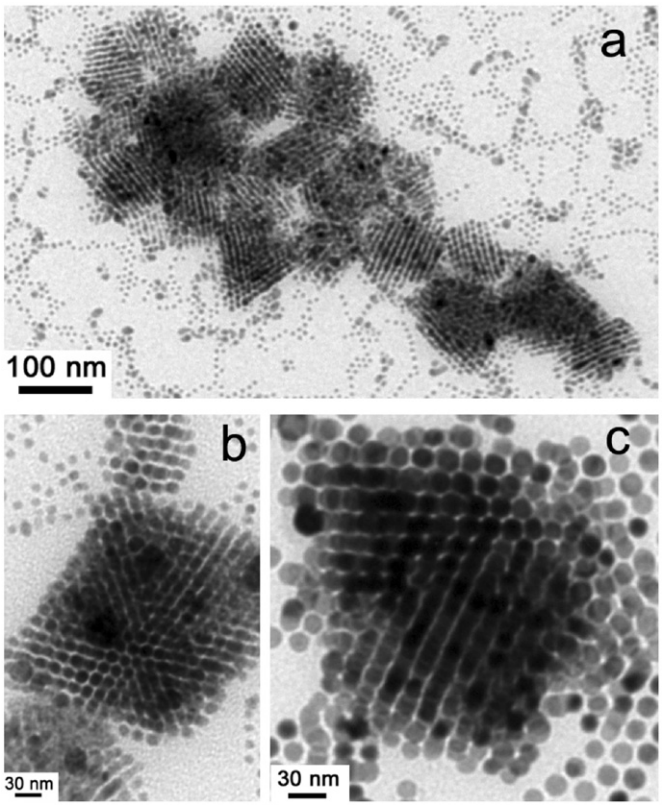

Fig. 10. TEM images of superlattice structures of (a, b) sample A and (c) sample C obtained at 100 min.

molecule can be evaluated from the following empirical equation: l (nm)$=0.25+0.127n$, where n is the number of $-CH_2-$ unit (for DDT, $n=12$), thus the length of DDT molecule is calculated to be about 1.77 nm [39]. Therefore, the average distance between two neighboring Ag nanospheres is less than two folds of the DDT length. This result indicates that the adsorbed thiolates distributed on the surface of two adjacent nanospheres interdigitate with each other, which contributes to the formation of superlattice structures of the Ag nanospheres [21]. For samples A and C, the Ag nanospheres can also be self-assembled into highly ordered multilayered superlattice structures by adjusting the nanocrystal concentration and the speed of the solvent evaporation, and the TEM images for typical multilayered superlattice structures of samples A and C are shown in Fig. 10. Different-shaped 3D superlattices can be found and each 3D superlattice is made up of ordered close-packed nanospheres with different size. On the edge of these 3D superlattices, some monolayered superlattices are observed, in which the superlattice structures are followed by hexagonal close packing structure. According to the aforementioned results in combination with previous cases, the bundling and interdigitation of thiolate molecules on Ag nanospheres is favorable greatly to the self-assembly of Ag nanospheres [21]. On the other hand, the synergistic effects of the steric repulsions, the van der Waals attraction and directional dipolar interactions are not excluded in the formation of highly ordered superlattice structures.

4. Summary

In conclusion, high-quality Ag nanospheres with uniform size have been successfully synthesized through a one-pot process, which does not need pre-synthesis of single source precursors. Ag-thiolate precursor forms at the early stage of the reaction and its decomposition leads to further nucleation and growth of Ag nanospheres. During this process, the absorption spectra were employed to monitor the growth of Ag nanospheres. The size of the Ag nanospheres can be tuned by simply changing the experimental diameters such as reaction temperature, reaction time and the amount of Ag(Ac) added. The resultant Ag nanospheres can be self-assembled into highly ordered superlattice structures, which is independent on the particle size. The bundling and interdigitation of thiolate molecules adsorbed on the surface of Ag nanospheres may play an important role in the formation of superlattice structures of Ag nanospheres. This synthetic procedure is simple and highly reproducible, which may extend to prepare other inorganic functional nanocryatal. Furthermore, the resulting nanocrystals prepared using this method can be produced in a large scale, and it is important for industrial applications.

Acknowledgments

This work was partly supported by NSFC projects (60954001, 60825407, 60736034, 61076009 and 50990064), "973" projects (2010CB933800), Program for NCET (08-0717) and the "111" Project (No.B08002). S.Q. thanks the research fund from Key Laboratory of Photochemical Conversion and Optoelectronic Materials, TIPC, CAS. A.T. is also grateful to China Postdoctoral Science Foundation (201003148 and 20090460499).

Appendix A. Supporting information

Supplementary data associated with this article can be found in the online version at doi:10.1016/j.jssc.2011.05.041.

References

[1] C.B. Murray, C.R. Kagan, M.G. Bawendi, Annu. Rev. Mater. Sci. 30 (2000) 545.
[2] Q.J. Sun, Y.A. Wang, L.S. Li, D.Y. Wang, T. Zhu, J. Xu, C.H. Yang, Y.F. Li, Nat. Photonics 1 (2007) 717.
[3] A.W. Tang, F. Teng, S. Xiong, Y. Wang, B. Feng, Y.B. Hou, J. Electrochem. Soc. 155 (2008) K190.
[4] F.Q. Hu, Y.L. Ran, Z. Zhou, M.Y. Gao, Nanotechnology 17 (2006) 2972.
[5] N. Tian, Z.Y. Zhou, S.G. Sun, Y. Ding, Z.L. Wang, Science 316 (2007) 732.
[6] J.Y. Ouyang, C.-W. Chu, C.R. Szmanda, L.P. Ma, Y. Yang, Nat. Mater. 3 (2004) 918.
[7] A.W. Tang, S.C. Qu, Y.B. Hou, F. Teng, H.R. Tan, J. Liiu, X.W. Zhang, Y.S. Wang, Z.G. Wang, J. Appl. Phys. 108 (2010) 094320.
[8] J.L. Castro, J.F. Arenas, M.R. López-Ramírez, D. Peláez, J.C. Otero, J. Colloid Interface Sci. 332 (2009) 130.
[9] C.M. Shen, C. Hui, T.Z. Yang, C.W. Xiao, J.F. Tian, L.H. Bao, S.T. Chen, H. Ding, H.J. Gao, Chem. Mater. 20 (2008) 6939.
[10] Y.H. Kim, D.K. Lee, H.G. Cha, C.W. Kim, Y.S. Kang, Chem. Mater. 19 (2007) 5049.
[11] H.G. Liu, F. Xiao, C.W. Wang, Q. Xue, X. Chen, Y.I. Lee, J.C. Hao, J.Z. Jiang, J. Colloid Interface Sci. 314 (2007) 297.
[12] Y.X. Hu, J.P. Ge, D. Lim, T.R. Zhang, Y.D. Yin, J. Solid State Chem. 181 (2008) 1524.
[13] S.A. Harfenist, Z.L. Wang, M.M. Alvarez, I. Vezmar, R.L. Whetten, Adv. Mater. 9 (1997) 817.
[14] Y.B. Chen, L. Chen, L.M. Wu, Inorg. Chem. 44 (2005) 9817.
[15] Q. Tang, S.M. Yoon, H.J. Yang, Y. Lee, H.J. Song, H.R. Byon, H.C. Choi, Langmuir 22 (2006) 2802.
[16] Y.Z. Huang, W.Z. Wang, H.Y. Liang, H.X. Xu, Cryst. Growth Design 9 (2009) 858.
[17] Y. Yin, Z.Y. Li, Z. Zhong, B. Gates, Y. Xia, S. Venkateswaran, J. Mater. Chem. 12 (2002) 522.
[18] M.S. Bakshi, Langmuir 25 (2009) 12697.
[19] Y. Sun, Y. Xia, Science 298 (2002) 2176.
[20] F. Dumestre, B. Chaudret, C. Amiens, P. Renaud, P. Fejes, Science 303 (2004) 821.
[21] Z.L. Wang, S.A. Harfenist, R.L. Whetten, J. Bentley, N.D. Evans, J. Phys. Chem. B 102 (1998) 3068.
[22] Z.L. Wang, Adv. Mater. 10 (1998) 13.
[23] Y. Yin, A.P. Alivisatos, Nature 437 (2005) 664.

[24] Y. Wang, Y. Hu, Q. Zhang, J. Ge, Z. Lu, Y. Hou, Y. Yin, Inorg. Chem. 49 (2010) 6601.
[25] H.Z. Zhong, Y. Zhou, M.F. Ye, Y.J. He, J.P. Ye, C. He, C.H. Yang, Y.F. Li, Chem. Mater. 20 (2008) 6434.
[26] A. Manna, B.D. Kulkarni, Chem. Mater. 9 (1997) 3032.
[27] D.V. Leff, L. Brandt, J.R. Heath, Langmuir 12 (1996) 4723.
[28] A.W. Tang, S.C. Qu, K. Li, Y.B. Hou, F. Teng, J. Cao, Y.S. Wang, Z.G. Wang, Nanotechnology 21 (2010) 285602.
[29] N.K. Chaki, J. Sharma, A.B. Mandle, I.S. Mulla, R. Pasricha, K. Vijayamohanan, Phys. Chem. Chem. Phys. 6 (2004) 1304.
[30] N. Sandhyarani, M.R. Resmi, R. Unnikrishnan, K. Vidyasagar, S. Ma, M.P. Antony, G.P. Selvam, V. Visalakshi, N. Chandrakumar, K. Pandian, Y.T. Tao, T. Pradeep, Chem. Mater. 12 (2000) 104.
[31] D.G. Gastner, K. Hinds, D.W. Grainger, Langmuir 12 (1996) 5083.
[32] M.C. Bourg, A. Badia, R.B. Lennox, J. Phys. Chem. B 104 (2000) 6562.
[33] S.H. Choi, K. An, E.G. Kim, J.H. Yu, J.H. Kim, T. Hyeon, Adv. Funct. Mater. 19 (2009) 1645.
[34] M.B. Sigman, A. Ghezelbash, T. Hanrath, A.E. Saunders, F. Lee, B.A. Korgel, J. Am. Chem. Soc. 125 (2003) 16050.
[35] Y. Yang, S.M. Liu, K. Kimura, Angew. Chem. Int. Ed. 45 (2006) 5662.
[36] B.A. Korgel, S. Fullam, S. Connolly, D. Fitzmaurice, J. Phys. Chem. B 102 (1998) 8379.
[37] M.P. Pileni, J. Phys. Chem. B 105 (2001) 3358.
[38] S.I. Stoeva, B.L.V. Prasad, S. Uma, P.K. Stoimenov, V. Zaikovski, C.M. Sorensen, K.J. Klabunde, J. Phys. Chem. B 107 (2003) 7441.
[39] A. Taleb, C. Petit, M.P. Pileni, Chem. Mater. 9 (1997) 950.
[40] D.S. Sidhaye, B.L.V. Prasad, Chem. Mater. 22 (2010) 1680.
[41] A.B. Smetana, K.J. Klabunde, C.M. Sorensen, J. Colloid Interface Sci. 284 (2007) 521.